Supporting Information

Intelligent Polymer-MnO_2 Nanoparticles for Dual-Activatable Photoacoustic and Magnetic Resonance Bimodal Imaging in Living Mice

Xiaoming Hu,[a] Chen Zhan,[a] Yufu Tang,[a] Feng Lu,[a] Yuanyuan Li,[a] Feng Pei,[b] Xiaomei Lu,*[b] Yu Ji,[a] Jie Li,[a] Wenjun Wang,[c] Quli Fan*[a] and Wei Huang[a, b, d]

[a]*Key Laboratory for Organic Electronics and Information Displays (KLOEID) & Institute of Advanced Materials (IAM), Jiangsu National Synergetic Innovation Center for Advanced Materials (SICAM), Nanjing University of Posts & Telecommunications, 9 Wenyuan Road, Nanjing 210023, China. E-mail: iamqlfan@njupt.edu.cn;*

[b]*Key Laboratory of Flexible Electronics (KLOFE) & Institute of Advanced Materials (IAM), Jiangsu National Synergetic Innovation Center for Advanced Materials (SICAM), Nanjing Tech University (NanjingTech), 30 South Puzhu Road, Nanjing 211816, China. E-mail: iamxmlu@njtech.edu.cn;*

[c]*Key Lab of Optical Communication Science and Technology of Shandong Province & School of Physics Science and Information Engineering, Liaocheng University, Liaocheng 252059, China;*

[d]*Shaanxi Institute of Flexible Electronics (SIFE), Northwestern Polytechnical University (NPU), Xi'an 710072, China.*

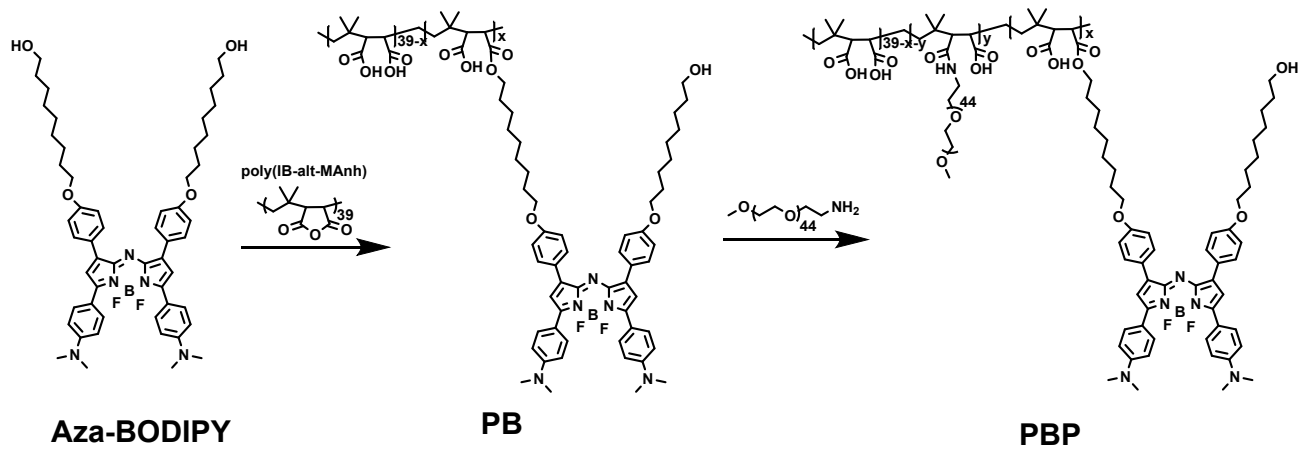

Scheme S1. Synthetic route to **PBP** polymer molecule.

Synthesis of PBP polymer molecule. Firstly, the near-infrared absorptive Aza-BODIPY molecule was first synthesized according to our previous study.[1] The Aza-BODIPY molecule was dried in a vacuum oven overnight. Then, 200 mg Aza-BODIPY and 5 mg LiH were dissolved in dried DMF (15 ml) under nitrogen and the solution was stirred overnight at room temperature. Next, a solution of 67 mg poly(isobutylene-alt-MAnh) (molecular weight (Mw) 6 kDa) dissolved in 5 ml dry DMF was added into above solution and continue to stir at room temperature. 12 h later, the crude product was acquired via evaporating under vacuum. As followed, the obtained amaranthine solid was dissolved in 10 mL deionized (DI) water and further purified by dialyzing in a dialysis membrane (M_w 7000 Da) with DI water for 3 days. And the solid of **PB** molecule was obtained in a lyophilizer.

100 mg **PB**, EDC·HCl (60 mg), NHS (40 mg), and NH_2-PEG (350 mg, M_w: 2000) were dissolved in 30 mL of dry DMF and stirred at room temperature. After 2 days, DMF was removed by reduced pressure distillation, and the residual solid was dissolved in appropriate amount of DI water. To remove unreacted NH_2-PEG and other impurities, the obtained solution was further purified by dialysis against water for 3 days with a dialysis bag (M_w 7000 Da). The final product (**PBP**) was dried by freeze-drying to acquire an amaranthine product.

The successful synthesis of the targeted molecule was confirmed by ^{1}H NMR spectra and UV-vis-NIR absorption spectra of **PBP**. By comparing and recording the typical resonance signal of PEG and Aza-BODIPY molecule (Figure S1) in the ^{1}H NMR spectrum of PBP (Figure S3), we can concluded that about 15 PEG chains and 12 BODIPY molecules are successfully linked to the polymer backbone.

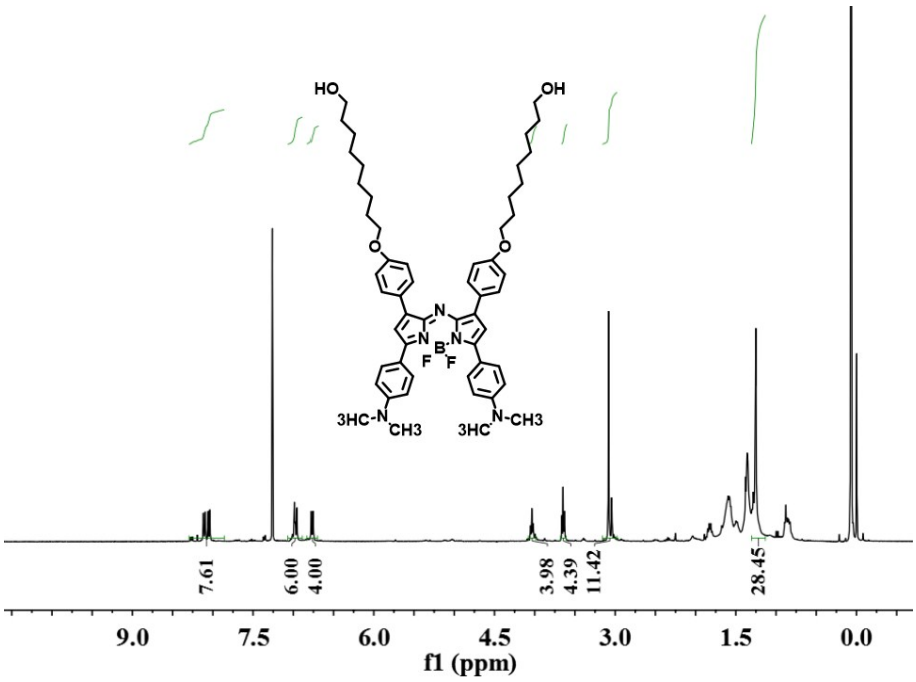

Figure S1. ^{1}H-NMR spectrum of **Aza-BODIPY**.

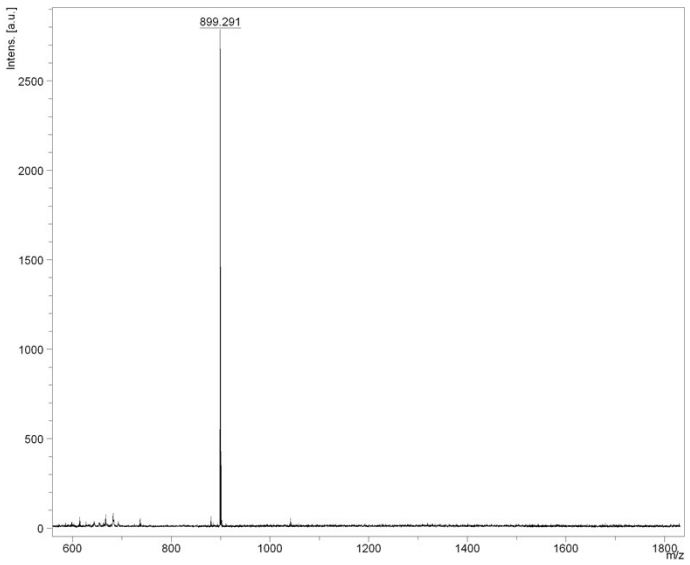

Figure S2. MALDI-TOF-MS spectrum of **Aza-BODIPY**.

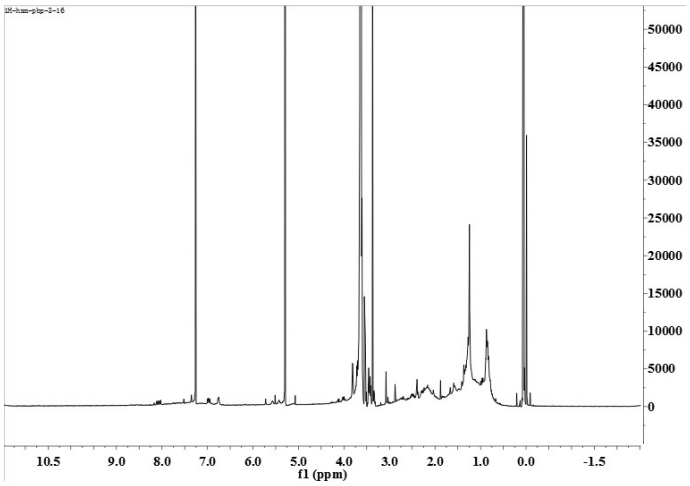

Figure S3. ^{1}H-NMR spectrum of **PBP**.

Table S1. GPC date of PBP in THF eluent.

Mn	Mw	Mw/Mn
46368	54714	1.18

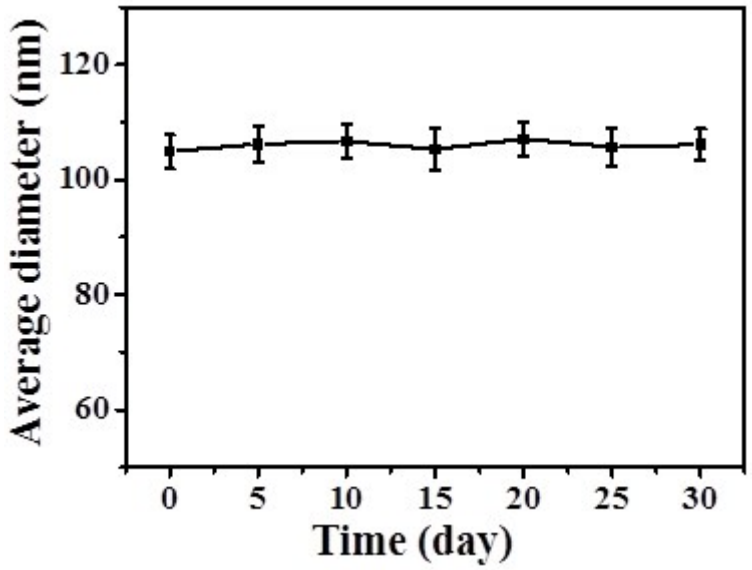

Figure S4. Average hydrodynamic diameters of the PBP@MnO_2 NPs stored in PBS for different time periods (0-30 days).

Physiological stability of PBP@MnO_2 NPs

The hydrodynamic size distribution of PBP@MnO_2 NPs in serum was performed to evaluate the stability of NPs in the biological environments. The PBP@MnO_2 NPs (MnO_2: 978 μg, PBP: 326 μg) were added to 50% fatal bovine serum (FBS, 5 mL) and 50% PBS (5 mL) and incubated at 37 °C for 48 h. The sample was analyzed at 0 h, 8 h, 24 h, and 48 h by DLS. As shown in Figure S5, all the hydrodynamic sizes of the NPs still retained at approximately 113 nm and their polydispersities were not changed. No obvious change in hydrodynamic sizes suggests the excellent physiological stability of PBP@MnO_2 NPs in biological environment.

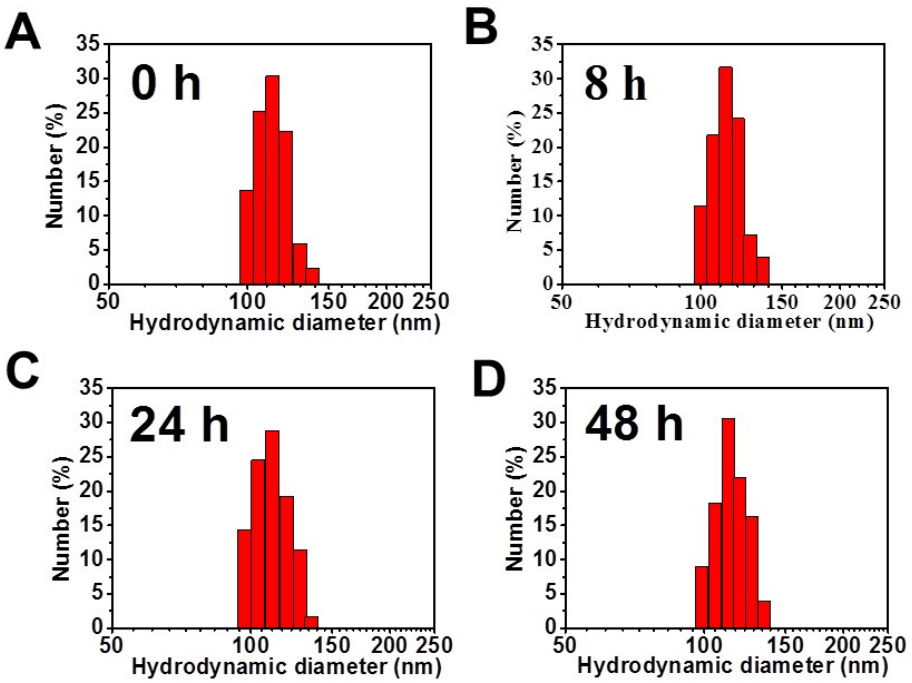

Figure S5. Stability of the PBP@MnO_2 NPs hydrodynamic size during different incubation periods (0, 8, 24 and 48 h) with serum.

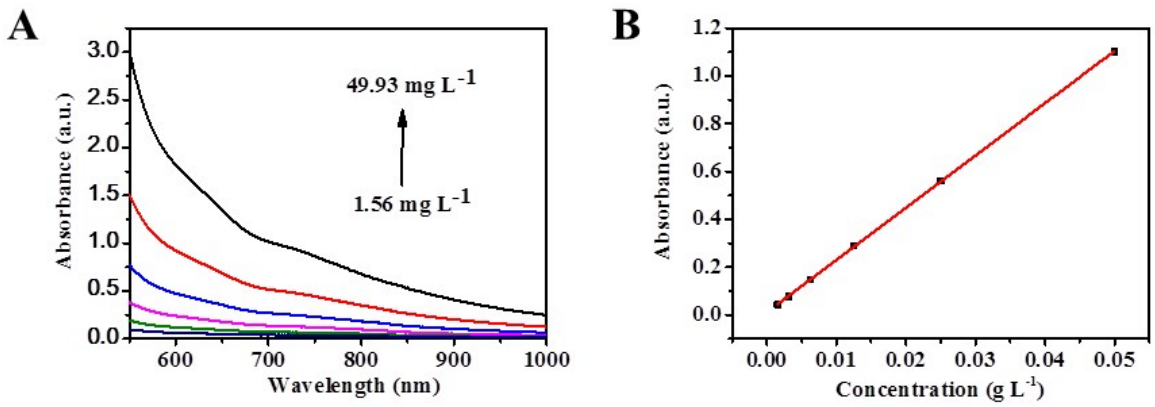

Figure S6. (A) Concentration dependence of the UV-vis-NIR absorbance of MnO_2 in PBS. The concentration of MnO_2 was measured by inductively coupled plasma mass spectrometry (ICP-MS). (B) The plot of absorbance density at 680 nm versus concentration. The straight line is a linear least-squares fit to the data, indicating the effective mass extinction coefficient of MnO_2 at the absorbance maxima. The mass extinction coefficient of MnO_2 at the 680 nm was 21.87 g^{-1} cm^{-1} L, which is higher than the widely used near-infrared (NIR) absorption gold nanorods (13.89 g^{-1} cm^{-1} L). The

excellent NIR absorption highlights the high potential of MnO_2 as NIR-responsive photoacoustic contrast or therapeutic agents.

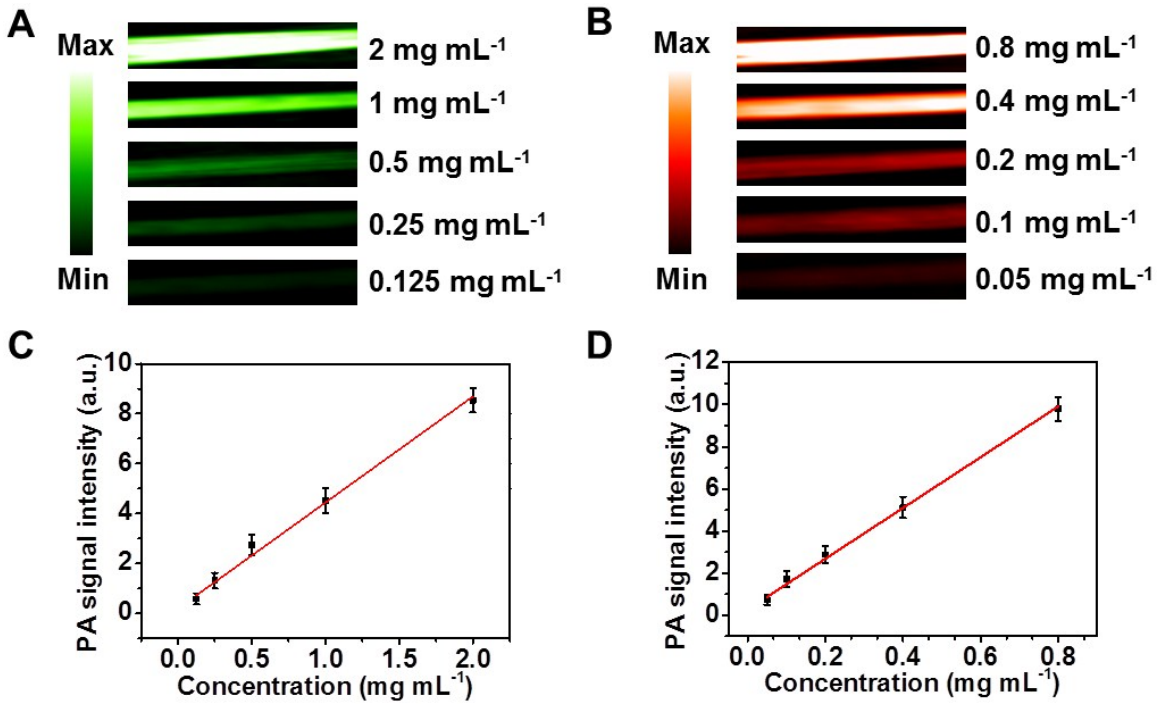

Figure S7. In vitro photoacoustic imaging capacity of MnO_2 NPs and PBP NPs. (A) In vitro PA images of MnO_2 NPs with varying contents ranging from 0.125 to 2 mg mL^{-1} recorded at 680 nm. (B) In vitro PA images of PBP NPs with varying contents ranging from 0.05 to 0.8 mg mL^{-1} recorded at 825 nm. (C) Linear dependence between the PA signals at 680 nm and concentrations of MnO_2 NPs. (D) Linear dependence between the PA signals at 825 nm and concentrations of PBP NPs.

For the sake of the optimal ratiometric PA response, the ideal integration ratio of PBP NPs and MnO_2 NPs was fixed at 1:3, in which the PA signals at 825 and 680 nm were tolerably unanimity.

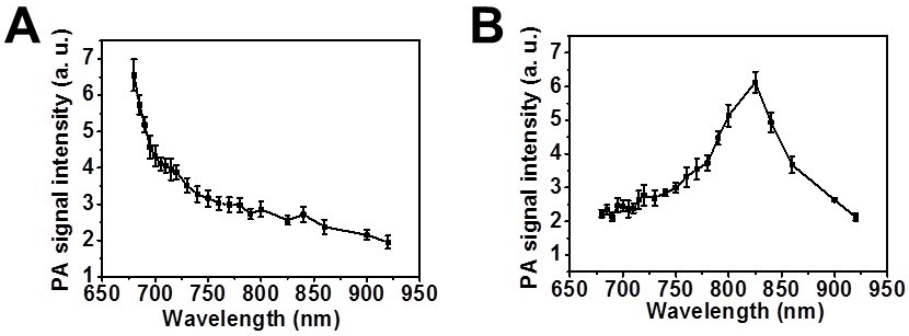

Figure S8. Representative in vitro PA spectra ranging from 680 to 920 nm of (A) MnO_2 NPs and (B) PBP NPs. MnO_2 NPs and PBP NPs possessed a PA signal spectrum ranging from 680 to 920 nm with peaks at 680 and 825 nm, respectively, which roughly fitted with the absorption spectra of them.

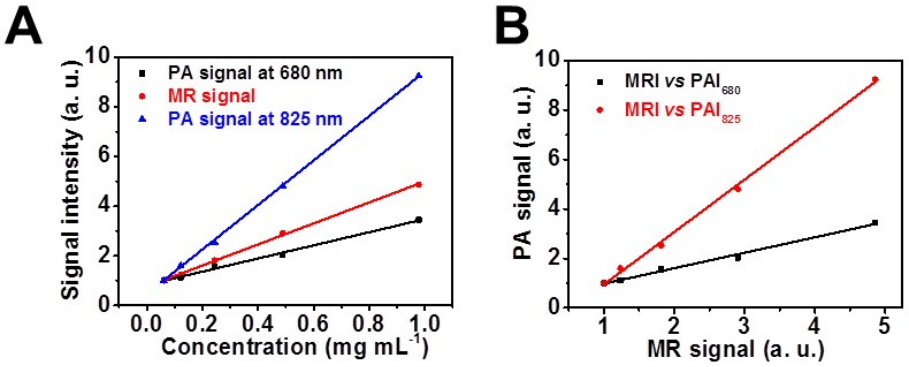

Figure S9. MRI-PAI signal correlation in vitro. (A) The relationship of MRI and photoacoustic signal with PBP@MnO_2 NPs concentration. (B) MR signal vs. PA signal.

We studied the relationship of MR versus PA signal intensity of the PBP@MnO_2 NPs and they showed good linear relationship. In addition, the slope of increased MR signal intensity with different concentrations was higher than that of PA signal intensity at 680 nm, indicating that the sensitivity of the activatable MR contrast agent PBP@MnO_2 NPs for MRI can be greatly improved.

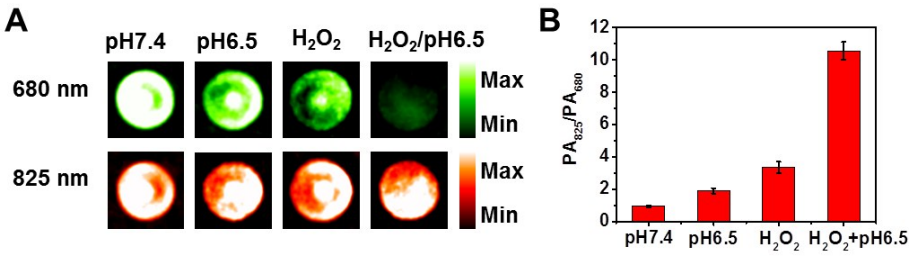

Figure S10. (A) PA images and (B) quantification of the ratiometric PA signals (PA_{825}/PA_{680}) of PBP@MnO2 NPs (PBP: 163 μg mL^{-1}, MnO_2: 489 μg mL^{-1}) in different conditions (H_2O_2: 100 μM).

In Vivo T_1-Weighted Magnetic Resonance Imaging

The in vivo MRI measurement was conducted at a Bruker Micro-MRI (7 T). Briefly, 4T1 neoplastic mice, intravenously administrated with PBP@MnO_2 NPs, were placed and imaged at the MR scanner. The parameters were TR/TE = 500/11 ms; field of view = 35 mm × 35 mm; flip angle = 30°; matrix, 256 × 256; and slice thickness = 1 mm.

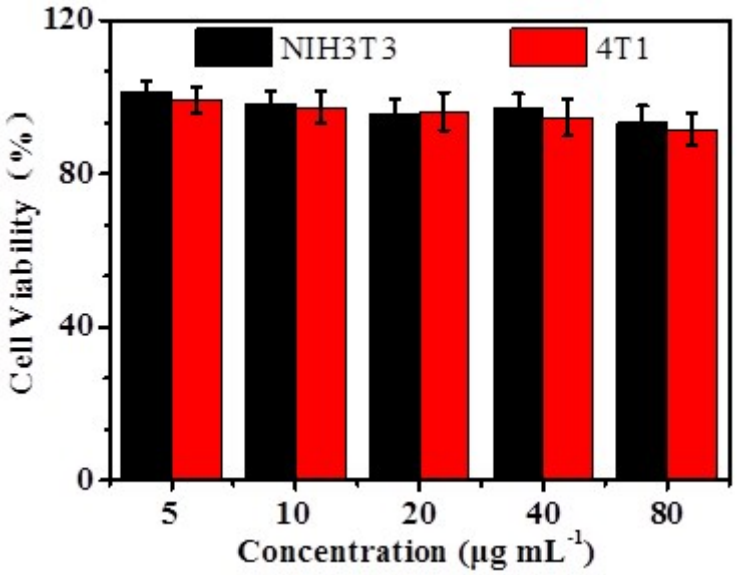

Figure S11. Cell viability of NIH-3T3 and 4T1 cells after incubation with PBP@MnO_2 NPs at different concentrations.